

## Geoimaging of subsurface fabric in Awgbagba, Southwestern Nigeria using geomagnetic and geoelectrical techniques

Lukman Ayobami Sunmonu <sup>a</sup>, Theophilus Aanuoluwa Adagunodo <sup>b,\*</sup>, Adetunji Ayokunnu Adeniji <sup>c</sup>,  
 Olumide Oyewale Ajani <sup>c</sup>

<sup>a</sup> Department of Pure and Applied Physics, Ladoke Akintola University of Technology, Ogbomoso, Nigeria

<sup>b</sup> Department of Physics, Covenant University, P.M.B. 1023, (Postal Code 112233) Ota, Ogun State, Nigeria

<sup>c</sup> Department of Physics and Solar Energy, Bowen University, P.M.B 284 Iwo, Osun State, Nigeria

\* Corresponding author: [theophilus.adagunodo@covenantuniversity.edu.ng](mailto:theophilus.adagunodo@covenantuniversity.edu.ng)

### Article history

Submitted 24 August 2017

Revised 10 September 2017

Accepted 2 January 2018

Published Online 13 June 2018

### Abstract

The heterogeneous nature of the earth has given rise to variations experienced in the subsurface. Some parts are good for hydrological exploration while others are good for civil engineering activities. These variations experienced in the subsurface could not be detected except through geophysical survey and analysis. Integration of ground magnetic and Vertical Electrical Sounding (VES) techniques were carried out in Awgbagba to image the subsurface fabric with a view to mapping subsurface geological features, such as the weak and competent zones, to determine the overburden thickness, and suitability of Awgbagba for civil engineering and hydrogeological purposes. Ten ground magnetic traverses were established in W-E and N-S azimuths. Twenty VES points were randomly sounded for the study in order to cover the entire study area. The magnetic residual field anomaly values ranged from -1, 600 to 700 nT. The study area is grouped into low, average, and high magnetic zones. The depth to magnetic sources ranged from 8.1 to 48.9 m with a mean value of 17.4 m. Three planar feature orientations in the study area are in NE-SW, NW-SE, and SE-NW orientations. VES results showed 7 QH-curve type, 6 HA-curve type, 4 KH-curve type, 1 AA-curve type, 1 HK-curve type and 1 QQ-curve type respectively. The ratio of thin-to-thick overburden and fresh-to-fractured bedrock are 3:7 and 2:3 respectively. It is concluded that the study area cannot withstand high-rise building constructions. However, the mapped fracture zones in the study area would serve as promising zones for borehole development.

**Keywords:** Bedrock mapping, civil engineering activities, geoimaging, geostructural features, ground magnetic, hydrogeological exploration, subsurface fabric, vertical electrical sounding

© 2018 Penerbit UTM Press. All rights reserved

## INTRODUCTION

Bedrock configuration mapping is crucial in civil engineering and hydrogeological settings. It helps to identify a suitable depth of building's foundation in civil engineering setting, while it assists the drillers to know the appropriate location and depth at which borehole needs to be drilled in hydrogeological setting. Telford et al. (1976) reported that subsurface investigation employing geophysical techniques provide very swift and cost effective channels of obtaining detailed subsurface geological information. Adewoyin et al. (2017) affirmed that "geophysical techniques can give volumetric measurements and produce images of the subsurface without physically disturbing the subsoil". There is need to carry out foundation studies in Nigerian present day because the rates at which structures fail are frightening and has become more severe (Adagunodo et al., 2014).

Apart from the fact that groundwater is the most abundant source of water available for human consumption, it is more advantageous as a source of potable water due to the fact that it is usually free from biological and chemical contaminants, it needs little or no purification before it can be used for domestic and industrial purposes. It is not easily affected by drought and odour while colouring is usually absent. The water has constant temperature and chemical composition. Suspended solutes (turbidity) are absent. It has far greater storage when compared to that of surface water. Groundwater occurs in geological

formations in the subsurface under hydrostatic pressure in the pores and cracks of rocks.

In addition, groundwater can be located in sedimentary terrain where it is less difficult to exploit except for its chemical composition. It can also be in the Basement Complex terrain where it can be a bit difficult to locate especially in areas underlain by crystalline unfractured or un-weathered rocks. Evidence has shown that geophysical methods are the most reliable and the most accurate means of all surveying method of subsurface structural investigations and rock variations (Carruthers, 1985; Emenike, 2001; Adewoyin et al., 2017; Adagunodo et al., 2017).

Ground magnetic technique requires measurements of the amplitude of magnetic components at discrete points along traverse distributed regularly throughout the survey area of interest. The theory and application that governs ground magnetic method has been reported by several researchers, among them include Adagunodo and Sunmonu (2012), Ojo et al. (2014), Adagunodo et al. (2015a) and Adagunodo et al. (2015b). However, Sunmonu et al. (2012) and Al-Khafaji and Al-Dabbagh (2016) have reported the theory of Electrical Resistivity (ER) and application of VES. Many researchers have employed ER mapping globally in order to identify and delineate different geoelectric layers. Of all varieties of the known geophysical prospecting methods, the electrical method remains the most widely used method. This applications range from engineering studies,

environmental assessment, to hydrogeological investigation. Roy (1972) reported that the chief advantage of the ER method is that quantitative modeling is possible using either computer software or published master curves. The resulting models can provide accurate estimates of depths, thicknesses, and electrical resistivity of subsurface layers. The layer electrical resistivity can then be used to estimate the electrical resistivity of the saturating fluid, which is related to the total concentration of dissolved solids in the fluid. Limitations of using the electrical resistivity method are largely due to site characteristics, rather than any other factors that may be caused due to the resistivity method or configuration used (Ojo et al., 2014).

Ground magnetic technique and VES have found a wide range of application in civil engineering and hydrogeological works (Al-Garni, 2009; Al-Amoush, 2010; Adelusi et al., 2013; Okwoli et al., 2014; Hewaidy et al., 2015; Olayanju et al., 2015; Adagunodo et al., 2017; Oyeyemi et al., 2017). These techniques are known as fast, high resolution, noninvasive, and cost effective techniques.

In view of the above, the ground magnetic method, and Vertical Electrical Sounding (VES) techniques were used to investigate the subsurface fabric of Awgbagba, southwestern Nigeria. The methods were therefore found relevant in the investigation of the area under study. The ground magnetic method was used to map possible planar features such as faults and fracture zones while VES was used to image the subsurface lithology of the study area.

**Geographical and geological settings of the study area**

The study area, Awgbagba is in Ola-Oluwa local government area of Osun State. It is bounded by Latitude 07° 42' 00" to 07° 42' 20" N and Longitude 04° 14' 55" to 04° 15' 22" E. It is accessible with major road leading from Iwo to Ikire Ile and Iwara (Fig. 1). The area under investigation experiences tropical rainfall, which dominates most of southwestern part of Nigeria. It has two distinct seasons; the wet season usually between the month of March and October and dry season which is between November and February. These two seasons define the climate of the study area. It falls within the Rainforest belt of Nigeria.

The study area is underlain by the Precambrian to Cambrian basement Complex of Osun state, southwestern Nigeria which are subdivided into Pan African (Older) Granitoids, metasediments/metavolcanic series, and migmatite gneiss complex. Awgbagba falls within Pan African (Older) Granitoids with quartz-syenite and banded gneiss as the major rocks around the study area. Fig. 2 is the representation of the geologic distribution around the study area.

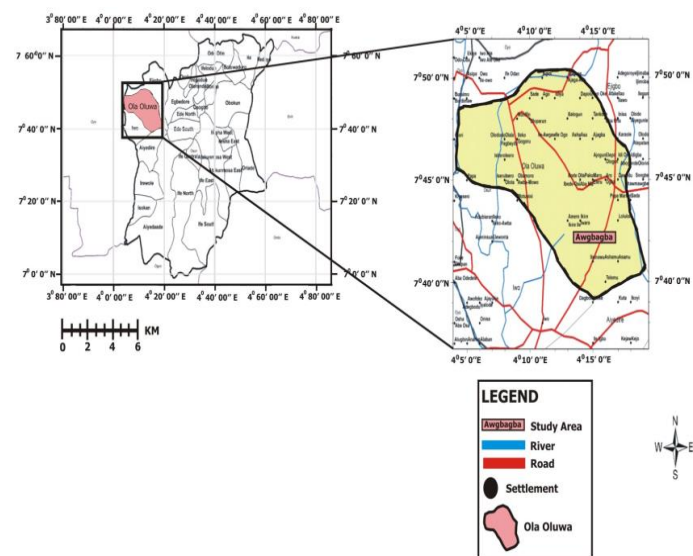


**Fig. 1** Map of Ola Oluwa local government area showing the study area, outset: map of Osun state showing Ola-Oluwa local government area.

**Materials and methods**

A proton precession magnetometer (GSM 19T) was used for the magnetic data acquisition while IGIS DDR1 Earth Resistivity meter and its accessories were used for the electrical resistivity data

acquisition. Ten traverses of ground magnetic profiling were occupied in north-to-south and west-to-east azimuths for the study. Twenty VES points were randomly sounded for the study in order to cover the entire study area (Fig. 3).

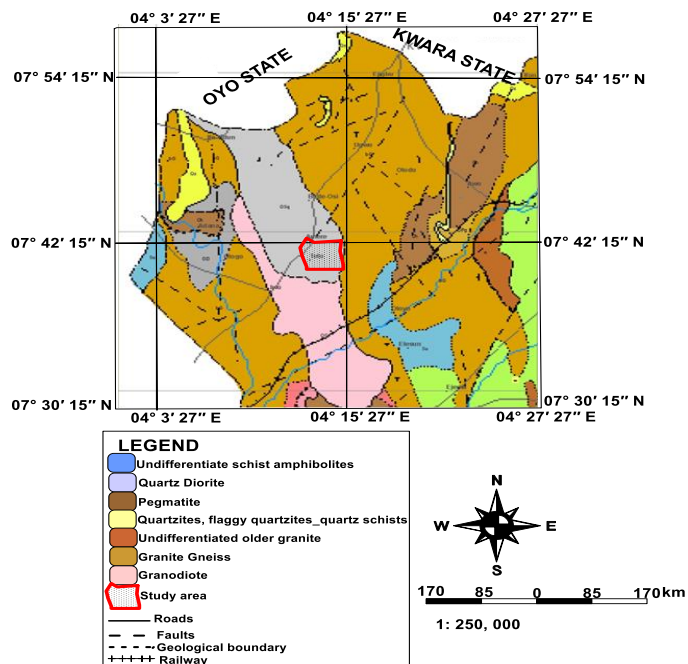


**Fig. 2** The Geological domains in some parts of Osun State showing the study area.

Ground magnetic data were drift corrected and presented as magnetic profiles of relative magnetic intensity values against distance and maps. Surfer 11 Software (Surfer 11 Software, 2012) was used to process the 2-D map of the study area. However, Peter-half slope method (Peters, 1949) was used to estimate relative depth to magnetic sources of the study area. The method has recently been used by Ojo et al. (2014). Automated Euler deconvolution technique was used to map the planar features and produce the geomagnetic sections from ground magnetic profiles in the study area.

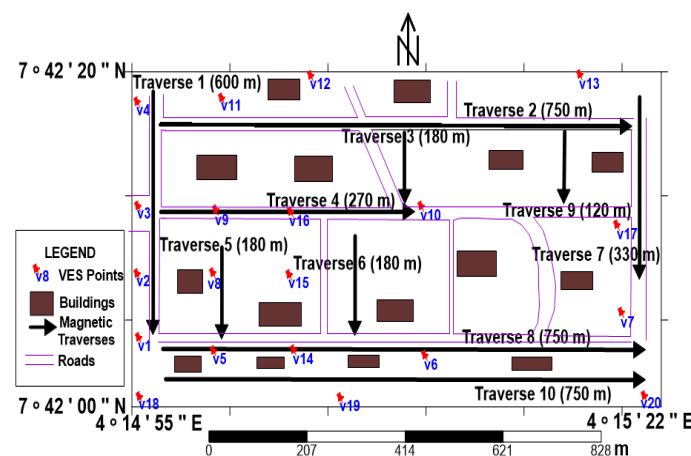


**Fig. 3** Base map of the study area.

The Schlumberger array was adopted for the field survey, with the maximum half-current electrode spacing (AB/2) varying from 65 to 100 m depending on the depth to bedrock and spread allowance. Geoelectrical sounding data were interpreted automatically using WinGLink software version 1.62.08 (WinGLink software, 2008), where the theoretical and auxiliary curves (Keller and Frishchnecht, 1966; Koefoed, 1979) were curve matched in order to obtain the resistivity values of different subsurface layers and their corresponding thicknesses and electrical resistivity of each layers. In order to have an

output results with low RMS values, the geoelectrical parameters obtained from WinGLink were further refined using a forward modeling computer algorithm, WinResist version 1.0 software (Vander Velpen, 2004). The geoelectrical results were presented as depth sounding curves, geoelectric sections, and maps (Adagunodo et al., 2013).

Integration of the ground magnetic and VES techniques would ensure adequate imaging of subsurface fabric in Awgbagba which would be useful for civil engineering and hydrogeological purposes. The profiles, sections and maps generated would enable the delineation of concealed geological structures.

## RESULTS AND DISCUSSION

### Ground magnetic interpretations

The Total Magnetic Intensity (TMI) of the study area is presented in Fig. 4. Apart from some pockets of low TMI values that are present towards the central, western, northern and eastern edges of the study area, the area generally depict high TMI values ranging from 28, 000 to 38, 000 nT. TMI is the combination of regional and residual field anomaly. However, this could not be used as the regional field tends to affect the local signatures of the investigated area. Therefore, after the regional field has been removed from TMI, the generated residual anomalies were used to produce the residual 2D contour map of the study area. This is presented in Fig. 5. The residual field anomaly ranged from -1, 600 to 700 nT. The study area is grouped into three residual magnetic zones. These are low magnetic zone ranging from -1, 600 to -900 nT, average magnetic zone ranging from -889 to -1 nT, and high magnetic zone ranging from 0 to 700 nT. A visual inspection of the residual map showed widely spaced contour lines in the study area which showed that the depth to quartzo-syenite and banded gneiss found in the study area are probably deeply seated. From Fig. 5, average-to-high magnetic values dominate the study area. However, the linear subparallel orientation of contour lines towards the northeastern, northwestern, and southern regions of the study area suggest shallow subsurface planar features in the study area.

Ten magnetic traverses were presented as magnetic profiles in Fig. 6a to 6j. Traverses 1, 3, 5, 6, 7 and 9 are in N-S azimuth while traverses 2, 4, 8 and 10 are in W-E azimuth. The lengths of these magnetic profiles are 600, 750, 180, 270, 180, 180, 330, 750, 120 and 750 m respectively. The magnetic profile interpretation is mostly preferred in local geological interpretation because geological details are easily revealed on profile presentations. Spikes were generally seen across the ten profiles in the study area. This could be due to the presence of subsurface magnetic bodies. Some spikes on the profiles could be interpreted as signatures of subsurface magnetic mineral rocks while the magnetic lows could be due to the presence of planar features such as fracture, rock contacts, or faults. From the rule of thumb, zones with magnetic highs are generally good for civil engineering purposes while the magnetic low zones are considered to be efficient for groundwater exploration.

The magnetic peaks on each profile were used to estimate depth to magnetic sources. The estimated depths derived from traverses 1 to 10 were summarized on Table 1.

From Table 1, mineral rocks with very thin, intermediate, and very thick bodies have their depths range as 22.1 m, 16.7 m and 13.3 m respectively. Based on Sunmonu et al. (2012) yardstick for estimating thin and thick overburden in a Precambrian Basement complex, the study area is generally underlain with thick overburden (that is, overburden thickness > 15 m). On the average, the depths to these mineral rocks from the surface ranged from 8.1 to 48.9 m. However, Peter did not specify from this method the shape of the buried body. He assumed that there could be a deformation of these mineral rocks due to some factors such as tectonic stress, weathering, water occurrence, pressure and temperature. He gave the possible geometry of the mineral rocks through the index values or proportionality factor. The shallower the depth, the thicker the body of the mineral rocks and the anomaly will be more pronounced and vice versa.

Ten geomagnetic sections were presented in Fig. 7a to 7j. These geomagnetic sections were generated from the weighted average of the

geology and geomagnetic signatures in the study area. The planar features were noticed on traverses 1, 5 and 7 which trend in NE-SW orientation, traverses 2, 8 and 10 which trend in NW-SE orientation, and traverse 3 which trend in SE-NW orientation. No planar feature was observed on traverses 4, 6 and 9. Banded gneiss was found as intrusive rocks beneath the overburden of traverses 2, 7, 8 and 10. Bedrock elevations and depressions were noticed across the geomagnetic sections which proved the heterogeneity nature of subsurface. Therefore, construction of high-rise buildings should not be encouraged along the fracture or rock contact mapped in Awgbagba. The average overburden thickness estimated in the study area (Table 1) also confirmed that construction of high-rise buildings in Awgbagba is unsafe. Fracture zones or rock contacts mapped in traverses 1, 2, 3, 5, 7, 8 and 10 are suggested zones for groundwater exploration.

Fig. 8 is the composite map of geomagnetic interpretation of Awgbagba. Low magnetic zone (blue colour) is scarcely noticed on the map except towards the northwestern part of the study area. Average magnetic zone (green and yellow colour) and high magnetic zone (orange and red colour) are found to be interwoven in distribution across the study area. General geomagnetic assessment of Awgbagba showed that it is incompetent for high-rise buildings. The orientation of fracture zone is essential in engineering and hydrogeological activities. It determines the direction of flow of water and buildings constructed against or perpendicular to the fracture zone is secured than the one constructed along or parallel to the fracture zone. From Fig. 8, part of northern, northeastern tips, eastern, southern and southwestern zones are safe for civil engineering purposes. Other zones are considered unsuitable for construction of high-rise buildings. Fracture zones/rock contacts were noticed in northwestern, northeastern, southeastern and southern zones of the study area (Fig. 8). If these zones with planar features are properly explored, high yield of borehole drilled in such area would be feasible.

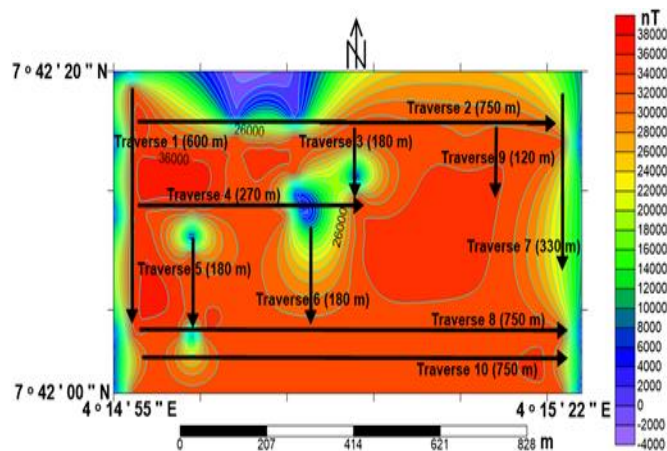


Fig. 4 The Total magnetic intensity map of the study area.

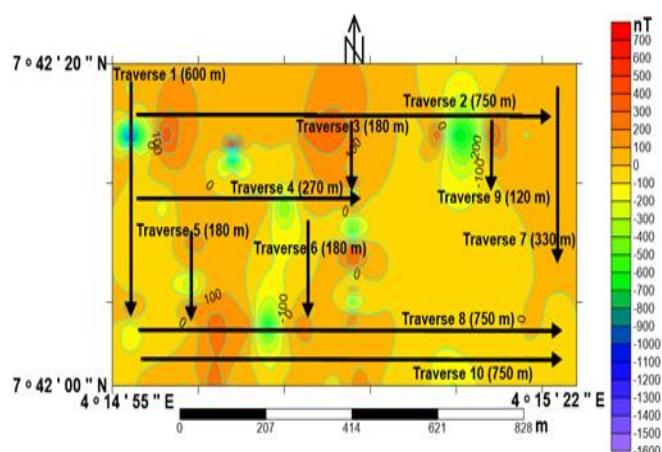


Fig. 5 The 2D Residual map of the study area.

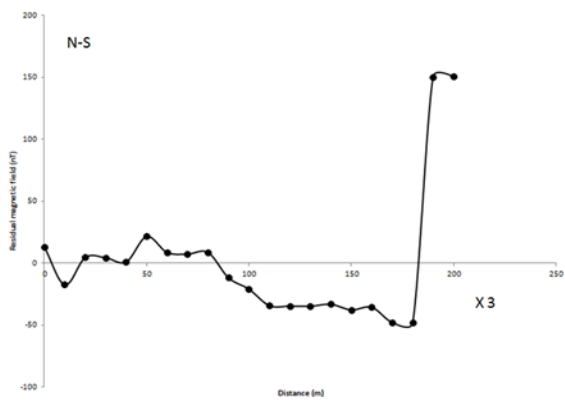


Fig. 6a Ground magnetic profile along traverse 1.

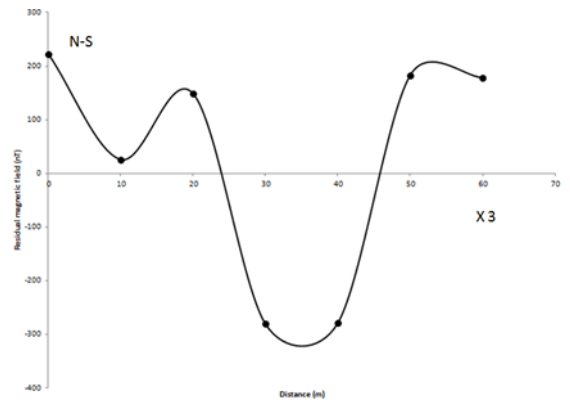


Fig. 6e Ground magnetic profile along traverse 5.

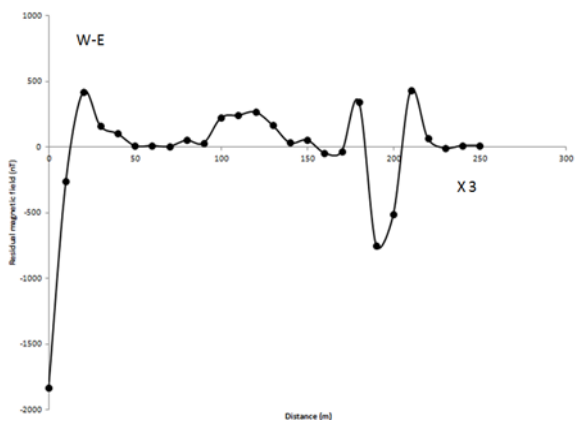


Fig. 6b Ground magnetic profile along traverse 2.

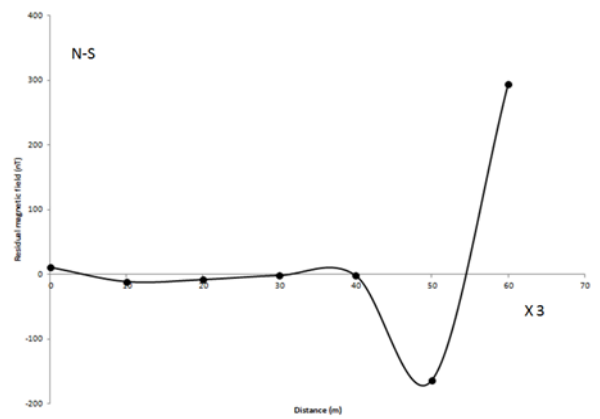


Fig. 6f Ground magnetic profile along traverse 6.

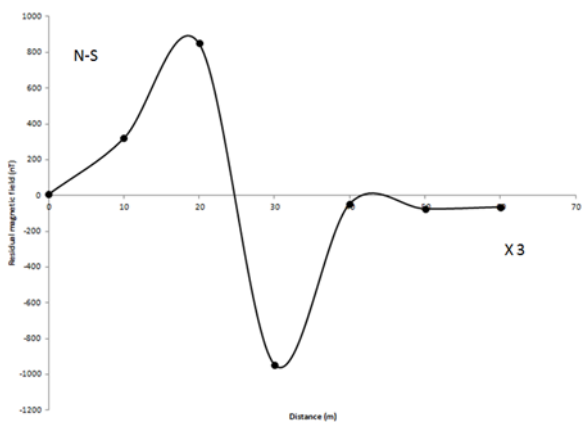


Fig. 6c Ground magnetic profile along traverse 3.

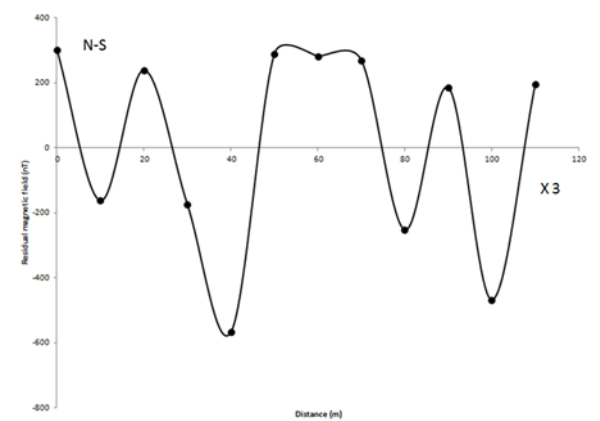


Fig. 6g Ground magnetic profile along traverse 7.

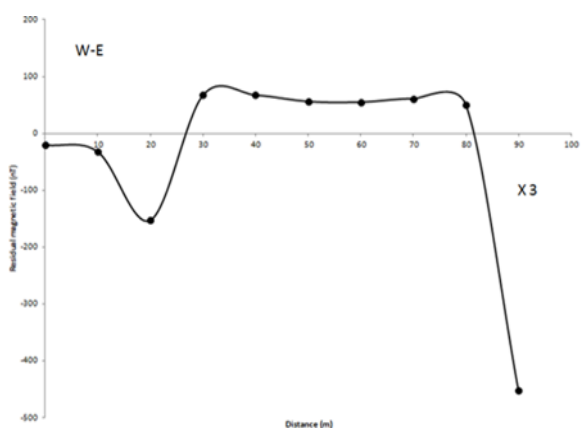


Fig. 6d Ground magnetic profile along traverse 4.

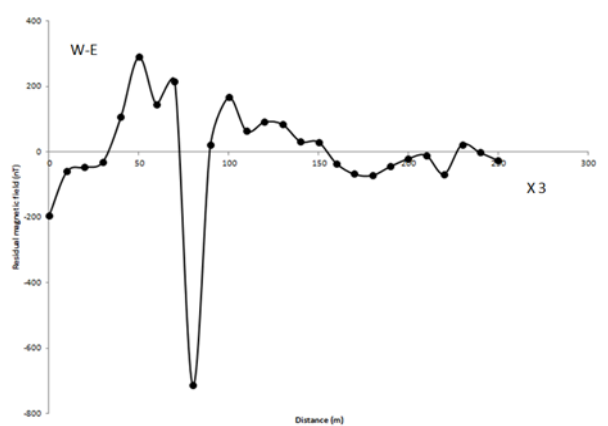


Fig. 6h Ground magnetic profile along traverse 8.

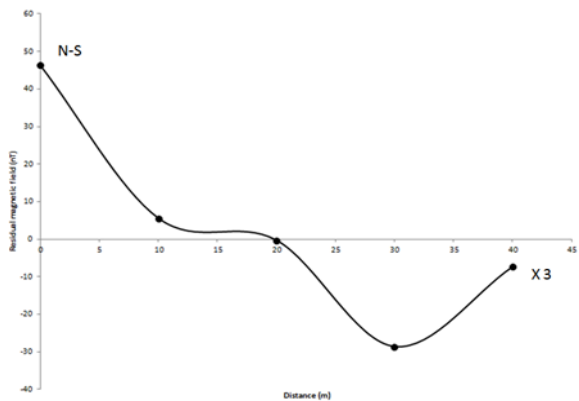


Fig. 6i Ground magnetic profile along traverse 9.

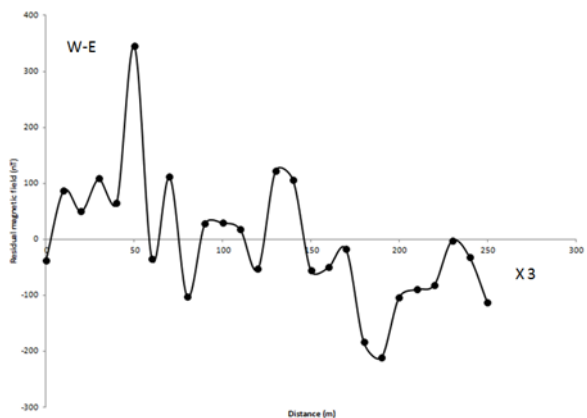


Fig. 6j Ground magnetic profile along traverse 10.

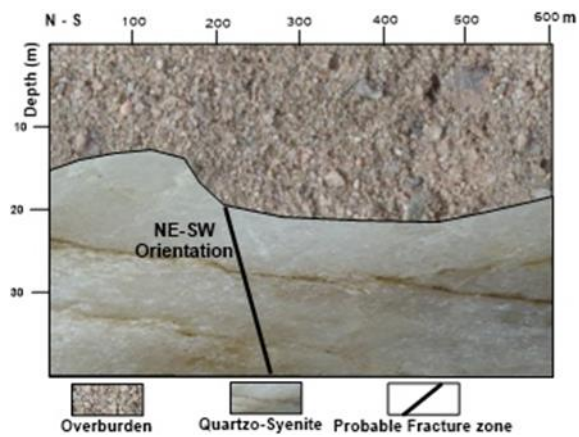


Fig. 7a Geomagnetic section of traverse 1.

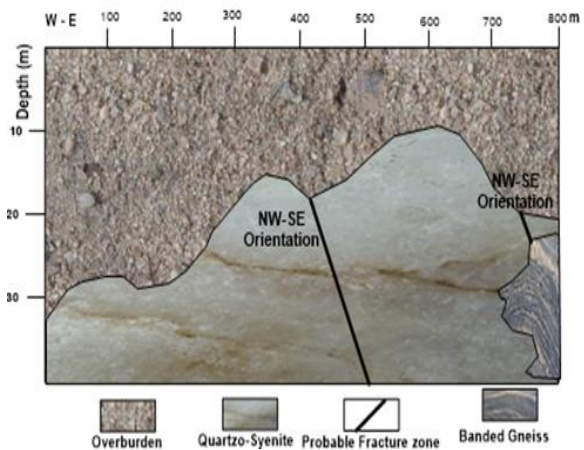


Fig. 7b Geomagnetic section of traverse 2.

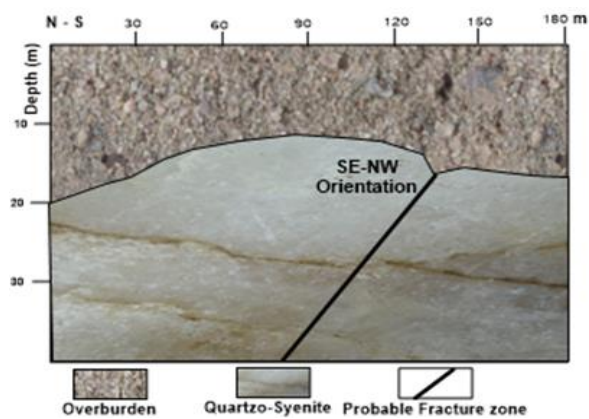


Fig. 7c Geomagnetic section of traverse 3.

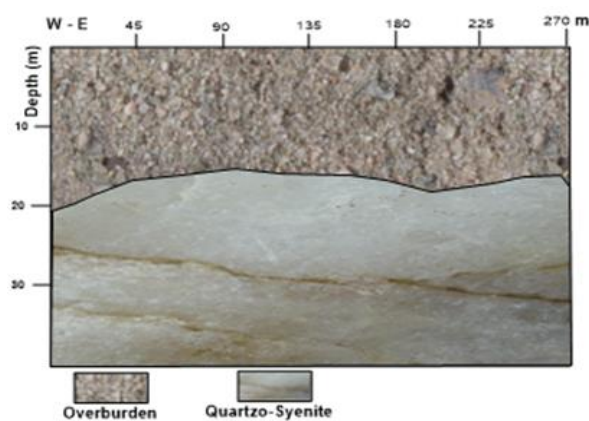


Fig. 7d Geomagnetic section of traverse 4.

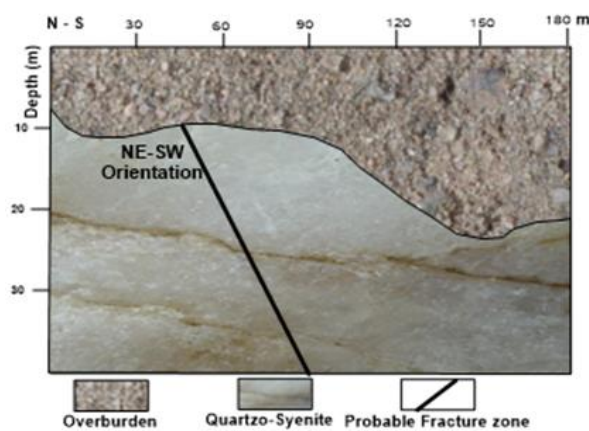


Fig. 7e Geomagnetic section of traverse 5.

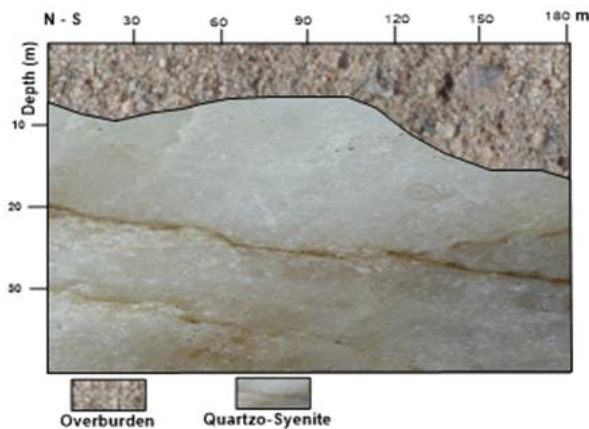
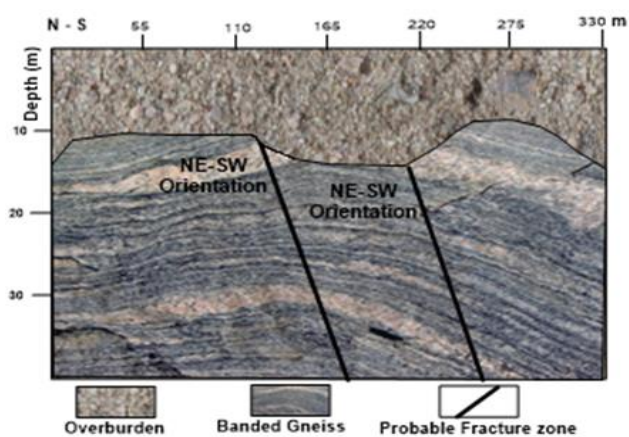


Fig. 7f Geomagnetic section of traverse 6.

**Table 1** Depth estimates of ground magnetic sources using Peter's half-slope method.

Profiles	Very thin body (m)	Intermediate thickness (m)	Very thick body (m)	Average (m)
1	20.1	15.0	12.0	15.7
	24.9	18.9	15.0	19.6
	24.9	18.9	15.0	19.6
2	37.5	28.2	22.5	29.4
	22.5	16.8	13.5	17.6
	15.0	11.4	9.0	11.8
	24.9	18.9	15.0	19.6
3	18.6	13.8	11.1	14.5
4	21.9	16.5	13.2	17.2
5	13.2	9.9	8.1	10.4
	24.9	18.9	15.0	19.6
6	10.2	7.8	6.3	8.1
	21.3	15.9	12.9	16.7
7	15.0	11.4	9.0	11.8
	18.9	14.4	11.4	14.9
	15.0	11.4	9.0	11.8
	19.5	14.7	11.7	15.3
8	24.9	18.9	15.0	19.6
	37.5	28.2	22.5	29.4
	16.8	12.6	10.2	13.2
	20.1	15.0	12.0	15.7
	20.1	15.0	12.0	15.7
9	62.4	46.8	37.5	48.9
	20.7	15.6	12.6	16.3
	16.2	12.3	9.9	12.8
10	24.9	18.9	15.0	19.6
	20.7	15.6	12.6	16.3
	23.7	17.7	14.4	18.6
	18.9	14.1	11.4	14.8
	12.6	9.3	7.5	9.8
	24.9	18.9	15.0	19.6
	16.8	12.6	10.2	13.2
20.7	15.6	12.6	16.3	
Mean	22.1	16.7	13.3	17.4



**Fig. 7g** Geomagnetic section of traverse 7.

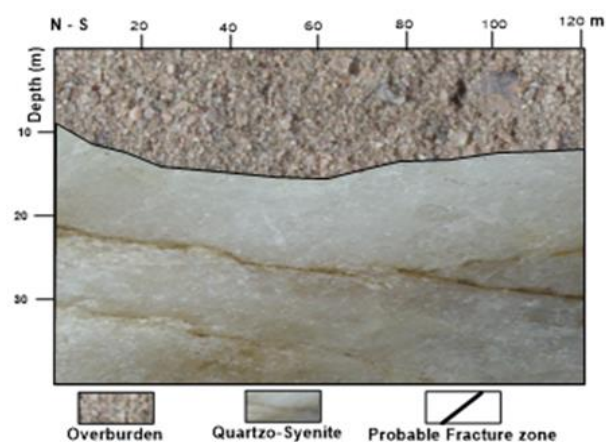


**Fig. 7i** Geomagnetic section of traverse 9.

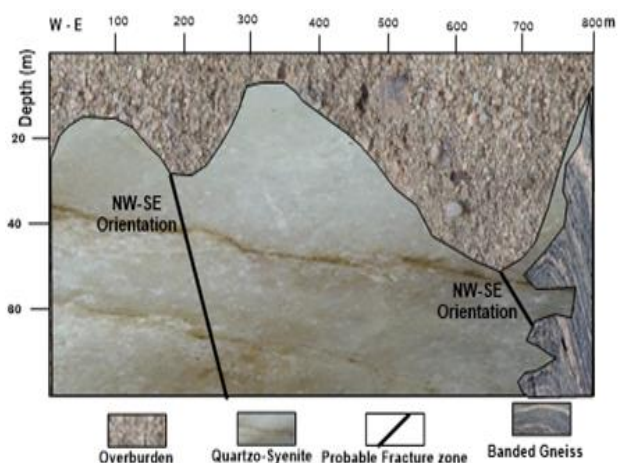


**Fig. 7h** Geomagnetic section of traverse 8.

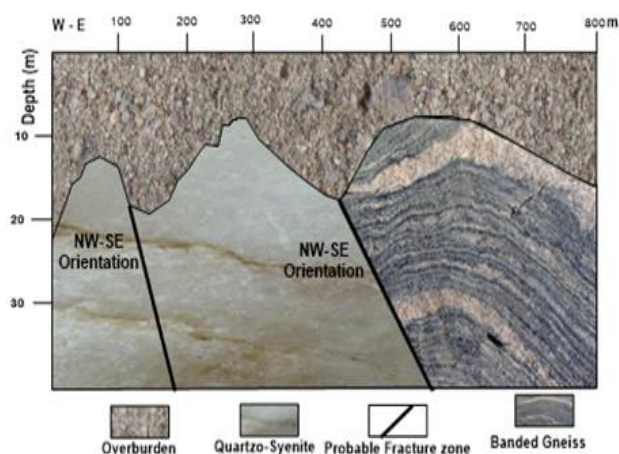


**Fig. 7j** Geomagnetic section of traverse 10.

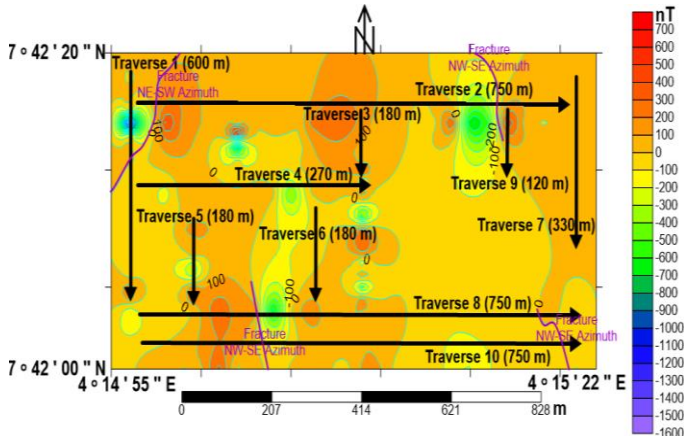


Fig. 8 Composite map of geomagnetic interpretation.

**Vertical electrical sounding interpretations**

The result of the VES data obtained from the field is presented as depth sounding curves (Fig. 9a to 9t), geoelectric sections (Fig. 10a to 10f), and geoelectric correlation (Fig. 11 to 13). However the qualitative interpretation applied to the quantitative interpretation results of the depth sounding curve enable the classification of the VES data into curve types according to Keller and Frishchnecht (1966) curve classification. All the VES curves are underlain with 4 – layered earth model. The VES curves types in the study area are QH, KH, HA, AA, HK, and QQ. 7 VES curves have QH, 6 VES curves have HA, 4 VES curves have KH, while AA, HK, and QQ type share 1 VES curve each.

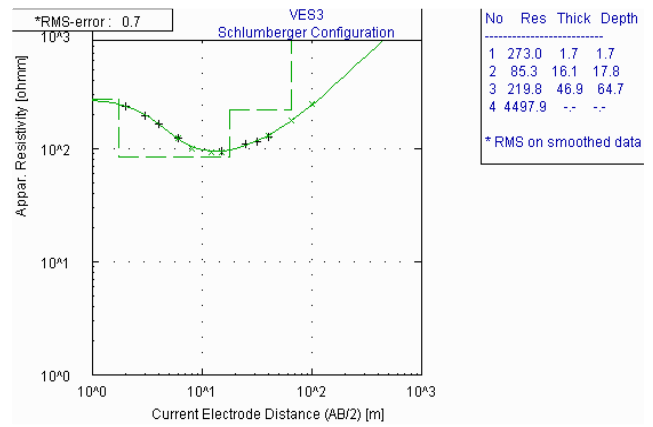


Fig. 9c VES curve 3.

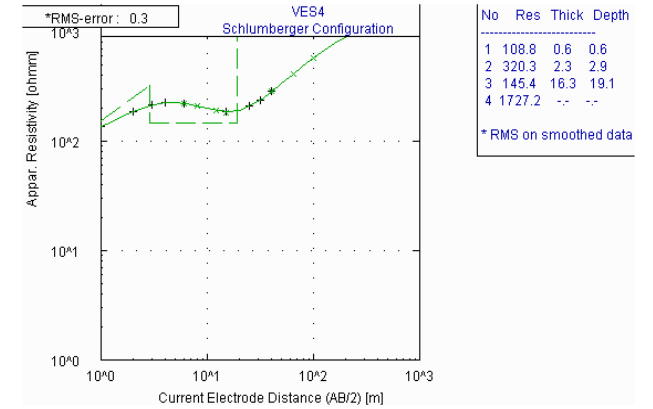


Fig. 9d VES curve 4.

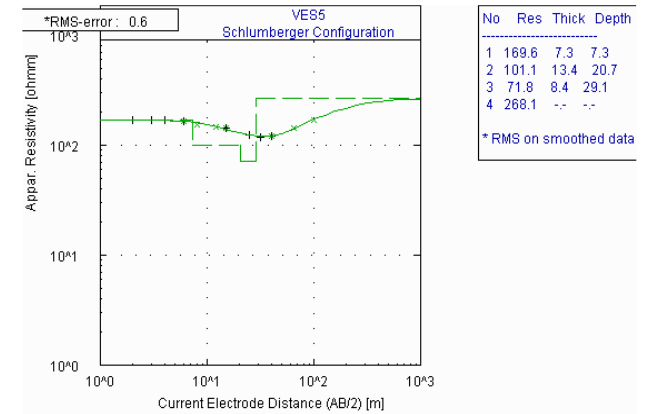


Fig. 9e VES curve 5.

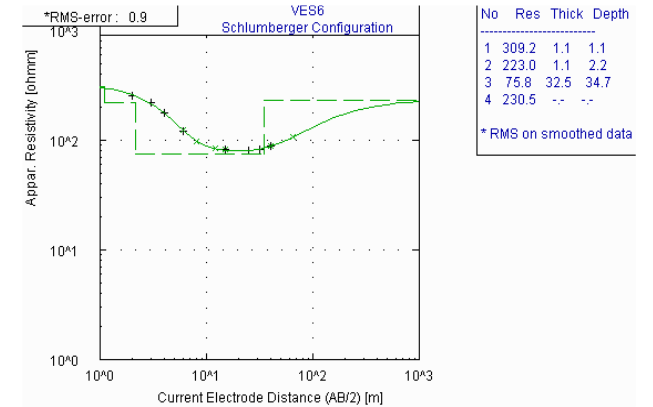


Fig. 9f VES curve 6.

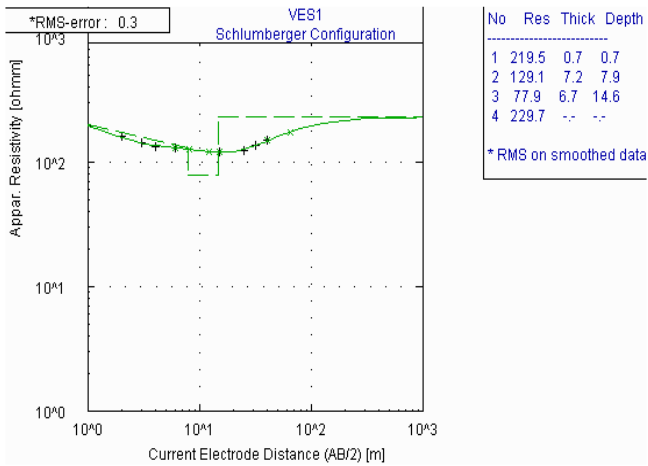


Fig. 9a VES curve 1.

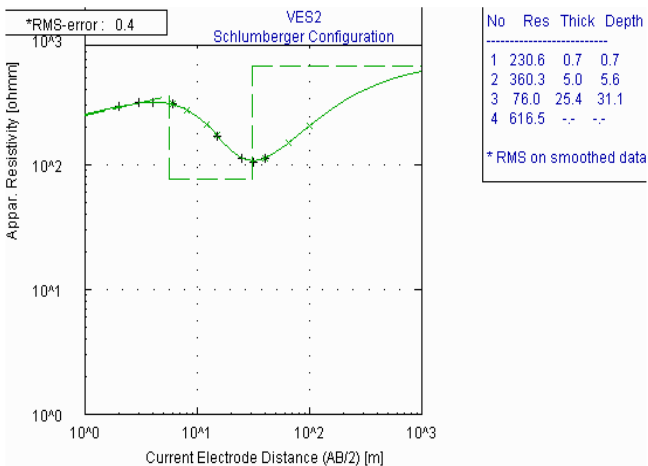


Fig. 9b VES curve 2.

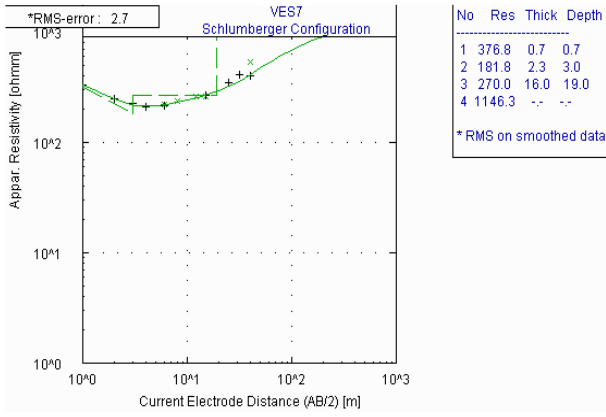


Fig. 9g VES curve 7.

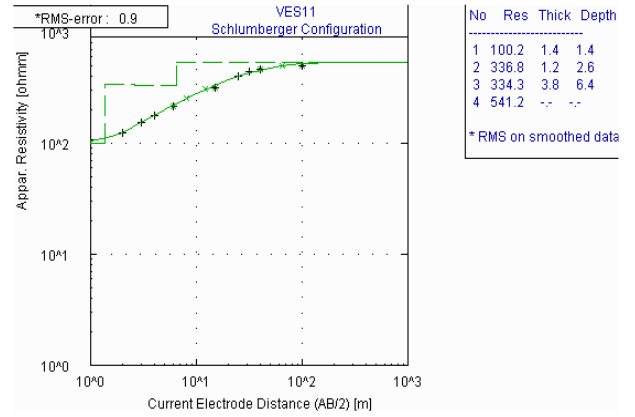


Fig. 9k VES curve 11.

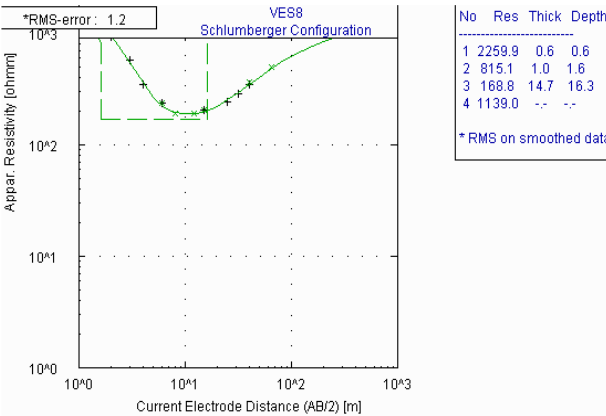


Fig. 9h VES curve 8.

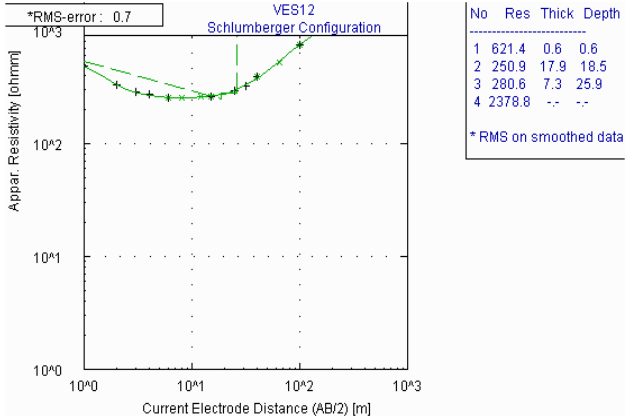


Fig. 9l VES curve 12.

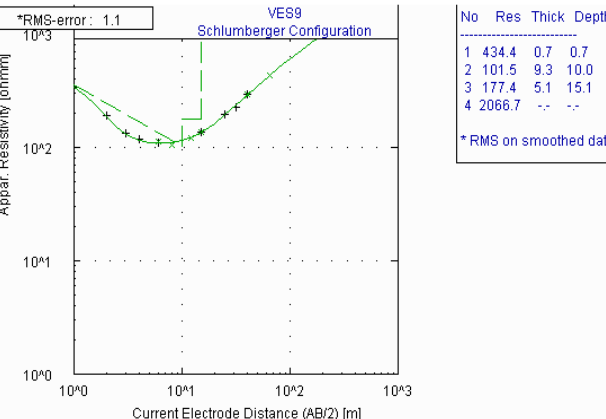


Fig. 9i VES curve 9.

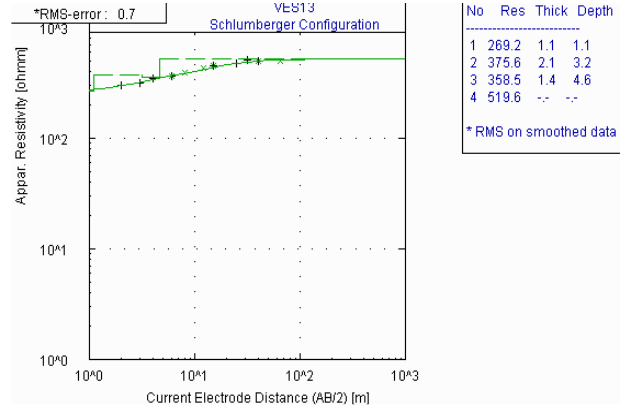


Fig. 9m VES curve 13.

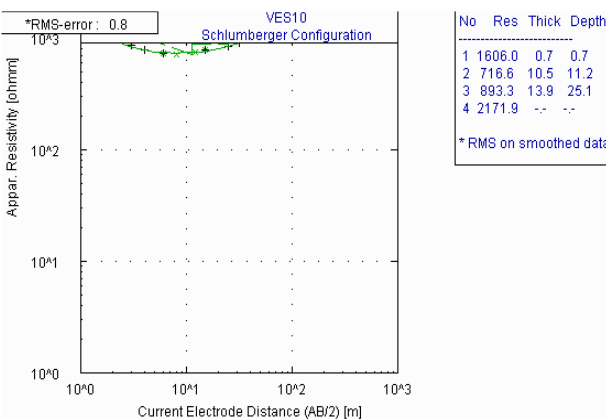


Fig. 9j VES curve 10.

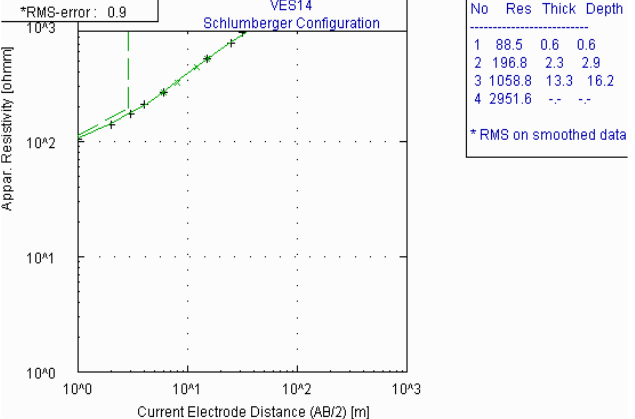


Fig. 9n VES curve 14.



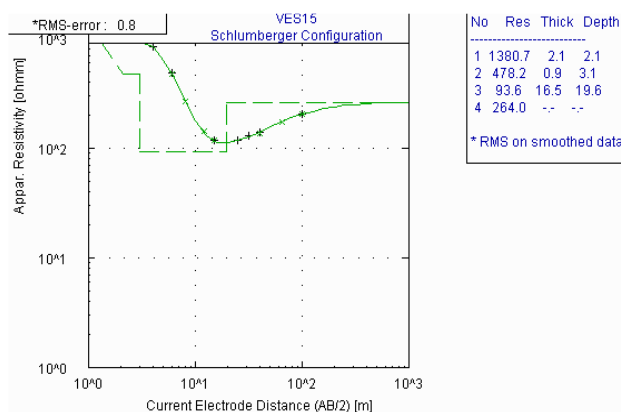


Fig. 9o VES curve 15.

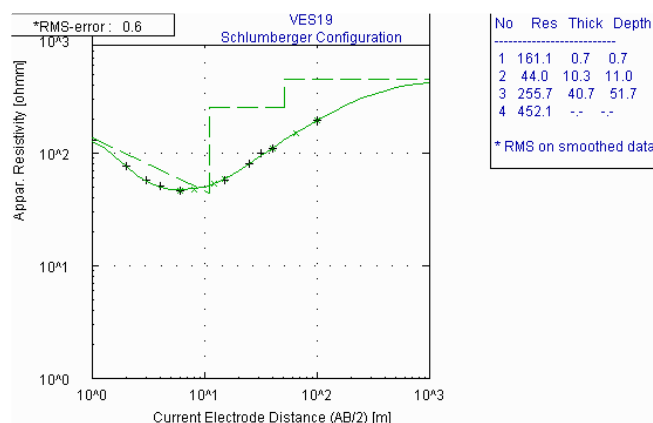


Fig. 9s VES curve 19.

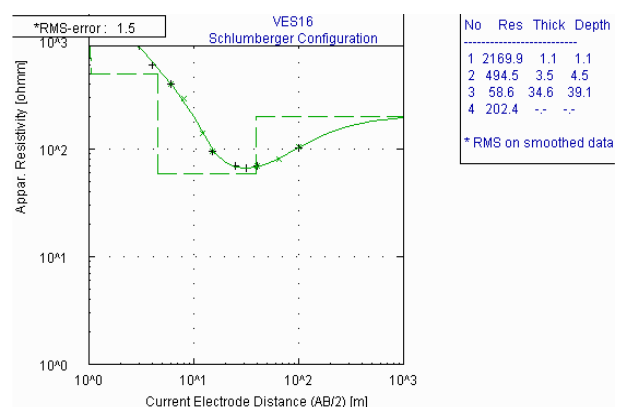


Fig. 9p VES curve 16.

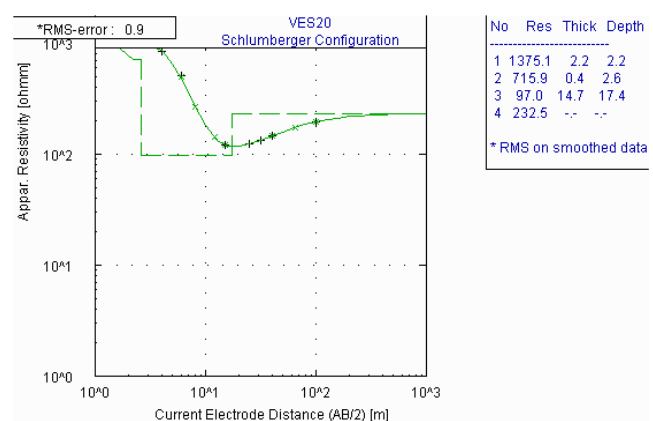


Fig. 9t VES curve 20.

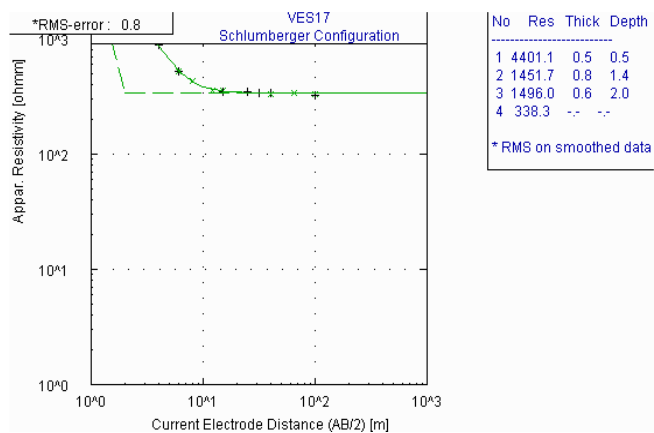


Fig. 9q VES curve 17.

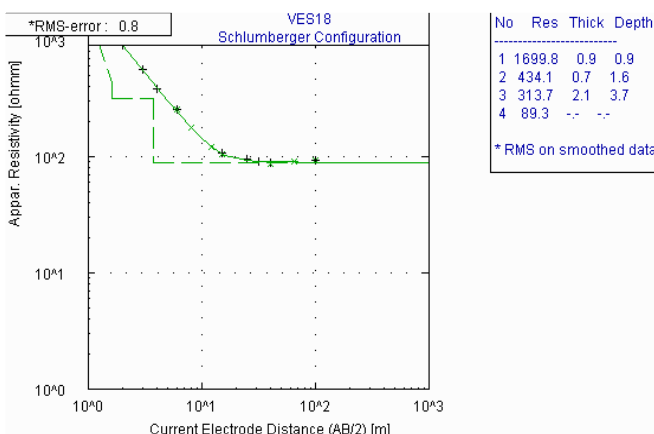


Fig. 9r VES curve 18.

The results of the interpreted VES curves were used to draw 2D geoelectric sections (Fig. 10a–f) along six profilesto show the vertical distribution of resistivity within the volume of the earth in the investigated area. The sections consist sequence of uniform horizontal (or slightly inclined) layers (horizons). Each layer (horizon) in a geoelectrical section may completely be characterized by its thickness and true resistivity. The geoelectrical sections showed both vertical and lateral variations in layer resistivity. One of the importances of 2D geoelectrical sections is that it helps someone to see clearly the variations in overburden thickness and the nature of each stratum.

Fig. 10a showed the geoelectrical section along profile 1. The section has geoelectrical formation equivalent of VES 1, VES 2, VES 3, and VES 4. This geoelectrical section has four layers. These layers are: topsoil, clay, weathered layer, and fractured or fresh basement. The topsoil is generally thin. The second layer constitutes the weathered layer which is indicated by the brown colour and is thick towards the central part of the section. This layer shows a ‘V-Shape’ in appearance. Clay (represented by yellow colour) is observed to intercalate with the weathered layer. This is observed from southern part through the central portion of the section. It seems that the clayey layer intruded in from the southern part of the geoelectrical section. Beneath these layers lie either fractured or fresh basement which serves as ground floor for these strata. High-rise building could only be built at the northern part of this section while it will take special consideration for the same high-rise building to be built in other parts of this section. This is because of the extremely thick overburden at the central part of the section and the fractured basement that extends from the southern part to some meters before reaching the central part of the section. However, this geoelectrical section seems to be favourable for groundwater exploration (hand-dug wells and boreholes) except at the northern part where only hand-dug wells could be favourable.

Fig. 10b showed the geoelectrical section along profile 2. The section has geoelectrical formation equivalent of VES 5, VES 8, VES 9, and VES 11. This geoelectrical section has four layers. These layers are: topsoil, lateritic zone, clay, weathered layer, and fresh or fractured

basement. The first layer constitutes the topsoil and the lateritic zone. Laterites are weathered material composed principally of the oxides of iron, aluminum, titanium, and manganese. Laterite ranges from soft, earthy, porous soil to hard dense rock. Only the central portion of this section shows the tendency to withstand high-rise building naturally. However, the two flanks of the section are underlain with fractured basement which could be dangerous for construction of high-rise buildings without building engineer's advice. Since groundwater exploration is favourable in crystalline bedrocks only at where there is thick overburden and/or fractured basement, hand-dug wells and boreholes could be successful at the both flanks of the section while only hand-dug well is advisable towards the central region of this section.

Fig. 10c showed the geoelectric section along profile 3. The section has geoelectrical formation equivalent of VES 14, VES 15, VES 16, and VES 12. This geoelectrical section has four layers. These layers are: topsoil, lateritic zone, clay, weathered layer, and fractured or fresh basement. The first layer constitutes the topsoil towards the flanks of the section while the lateritic layer seems to have replaced the topsoil toward the central portion of the section. The lateritic soil has a distance 45 to about 120 m. Beneath the topsoil/laterite, there is weathered layer and clayey zone. The weathered layer is evenly distributed while the clay zone which looks like a capsule is directly enveloped under the weathered layer at the center of the section with distance of about 40 to 110 m. Beneath this central zone is the fractured basement while the flanks of this section is underlain by fresh basement (though with thick overburden towards the northern side of the section). Only the southern part of the section showed competency for high-rise building construction while others needs special consideration before high rise building could be constructed on it.

Fig. 10d showed the geoelectric section along profile 4. The section has geoelectrical formation equivalent of VES 6 and VES 10 only. This geoelectrical section has four layers. These layers are: topsoil, lateritic zone, clay, weathered layer, and fractured or fresh basement. The first layer constitutes the topsoil towards the southern part of the section, while the laterites seemed to have replaced the topsoil toward the northern part of the section. The weathered layer beneath the lateritic soil has thick overburden to a depth of about 25 m. The clay zone towards the southern part of the section is underlain by fractured basement, while the weathered layer towards the northern part of the section is underlined by fresh basement. This area is generally not competent enough for engineering activities due to relatively thick overburden unit except for special advice from building experts. Borehole drilling will be successful towards the southern part of the section, while hand-dug wells could fail due to the presence of aquitard above the fractured basement in the terrain. However, if the lateritic layer is chiseled, groundwater exploration could be favourable at the northern side of the geosection.

Fig. 10e showed the geoelectric section along profile 5. The section has geoelectrical formation equivalent of VES 7, VES 17 and VES 13. This geoelectrical section has four layers. These layers are: topsoil, lateritic zone, weathered layer, and fractured or fresh basement. The first layer also constitutes the topsoil and the laterites. The lateritic zone (three consecutive layers) from the middle tends to have a depth of about 5 to 10 m. The weathered layer is noticed at the flanks of the section. The southern part of the section is underlain by fresh basement while the central portion to the northern portion is underlain by fractured basement. Only the southern part of the section has prospects for engineering activities while other parts require special advice. However, hand-dug wells will be suitable at the southern part of the section while from central to the northern part of the section requires boreholes developments.

Fig. 10f showed the geoelectric section along profile 6. The section has geoelectrical formation equivalent of VES 18, VES 19 and VES 20. This geoelectrical section has four layers. T

these layers are: topsoil, lateritic zone, clayey zone, weathered layer, and fresh or fractured basement. The first layer also constitutes the topsoil and the laterites. The laterites were noticed at both flanks if the section. Beneath the topsoil and laterites, a cone-shaped weathered layer was observed. The apex of this layer extends up to 50 m depth. Clay zone seemed to have intruded into the weathered layer through

the eastern side of the section. This clayey zone extends to the central part of the section. However, this section is underlain by fractured bedrock. This might be disastrous for engineering activities but good for groundwater exploration based on the previous interpretation from profiles 1 to 5.

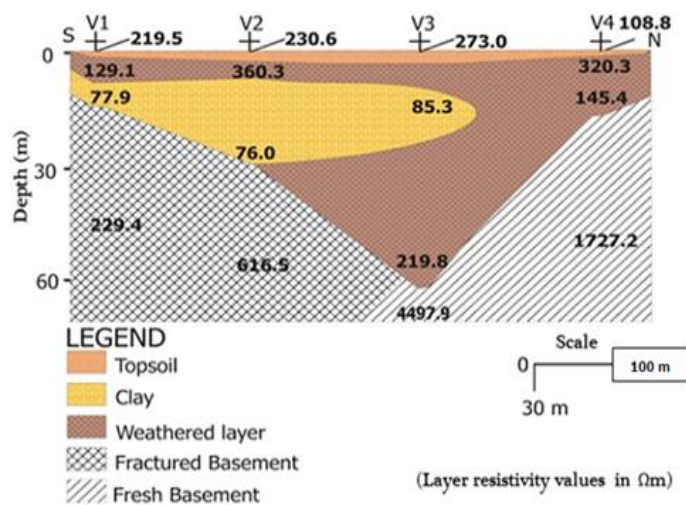


Fig. 10a Geoelectric section along profile 1.

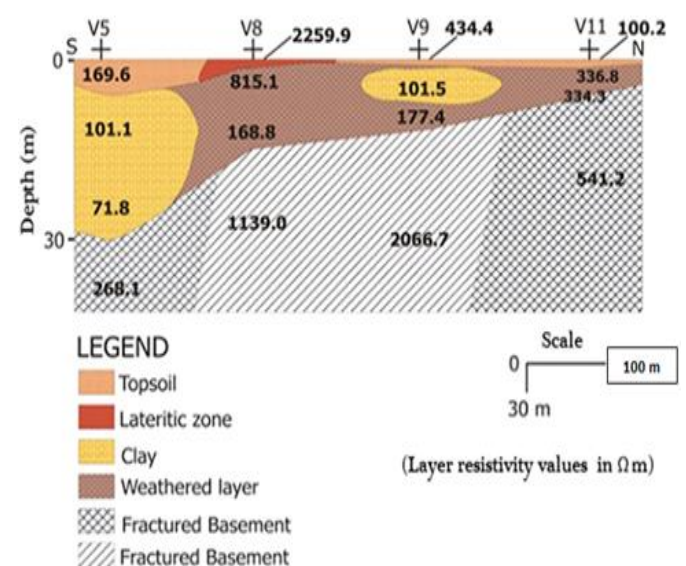


Fig. 10b Geoelectric section along profile 2.

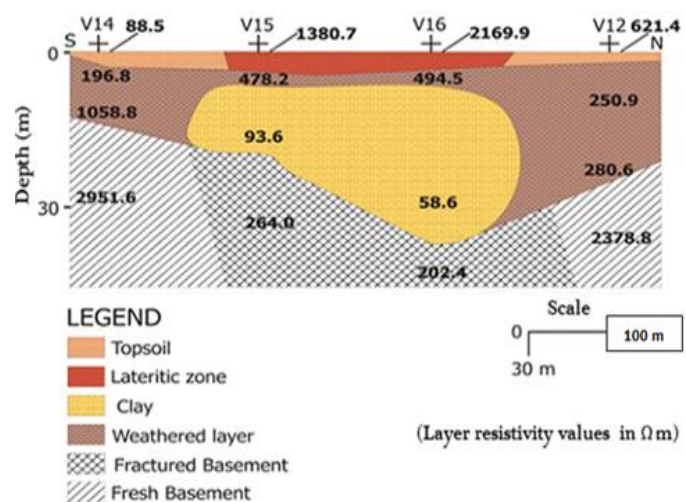


Fig. 10c Geoelectric section along profile 3.

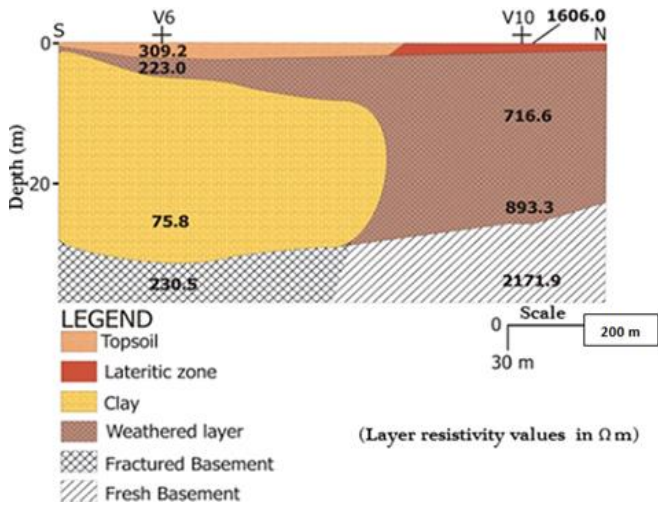


Fig. 10d Geoelectric section along profile 4.

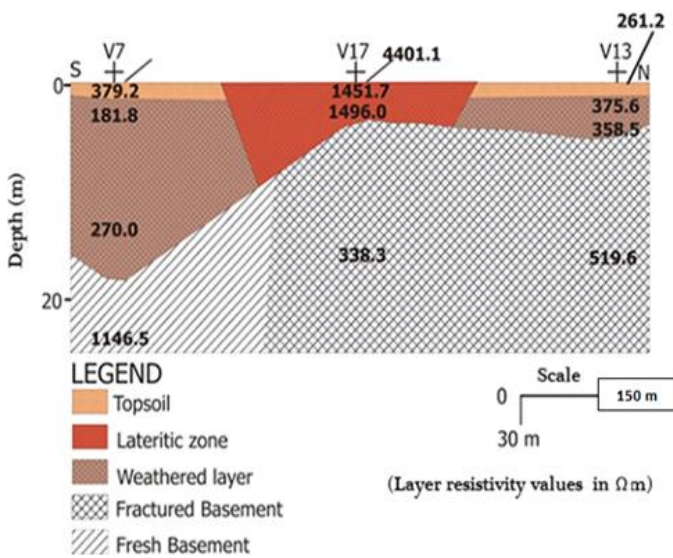


Fig. 10e Geoelectric section along profile 5.

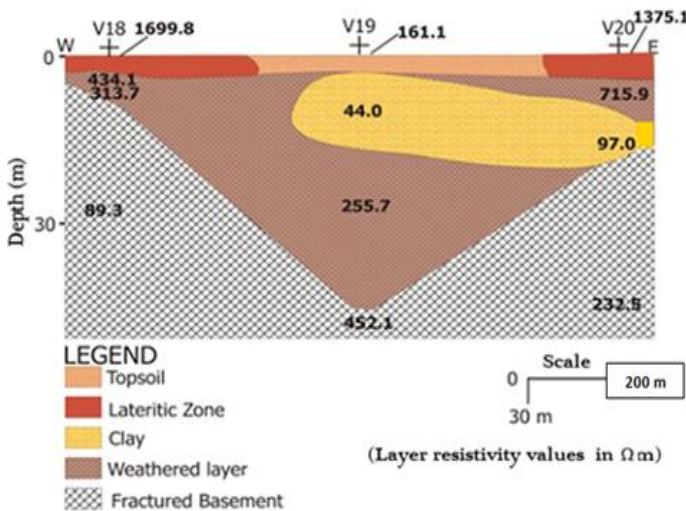


Fig. 10f Geoelectric section along profile 6.

Fig. 11 showed that six (6) VES stations have thin overburden (a depth less than 15 m) while fourteen (14) VES stations have thick overburden (a depth greater than 15 m). It was also observed that eight (8) VES stations are underlain by fresh bedrock while twelve (12) VES stations are underlain by fractured bedrock. This implies that: the ratio of thin to thick overburden is 3:7; the ratio of fresh basement to fractured basement is 2:3; and the average depth is 22.77 m.

Fig. 12a and b also showed the 2-D and 3-D maps of the overburden thickness in the study area. The yellow colour on the 2-D map represents the thin overburden while the cyan colour represents the thick overburden. The thin overburden is understood to favour high-rise building while the thick overburden should be avoided during foundation activities (except if the building experts are consulted for appropriate foundation type in such area) but it is considered favourable for groundwater activities.

However, Fig. 13a and b showed the 2-D and 3-D images/maps of the subsurface bedrock topography respectively. The yellow colour on the 2-D map represents the fresh bedrock while the cyan colour represents the fractured bedrock. There should be no fear of building on fresh bedrock because the fresh bedrock could act as protection for the building's foundation against the dynamic movement of the lithospheric plates. Since fractured bedrock is incompetent for engineering activities, construction of high-rise buildings should be encouraged on fresh bedrock zones.

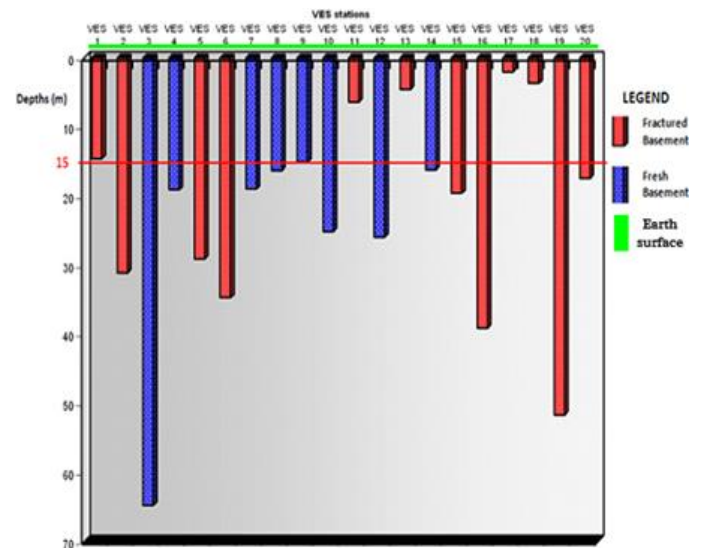


Fig. 11 Geoelectric evaluation of overburden thickness and basement nature.

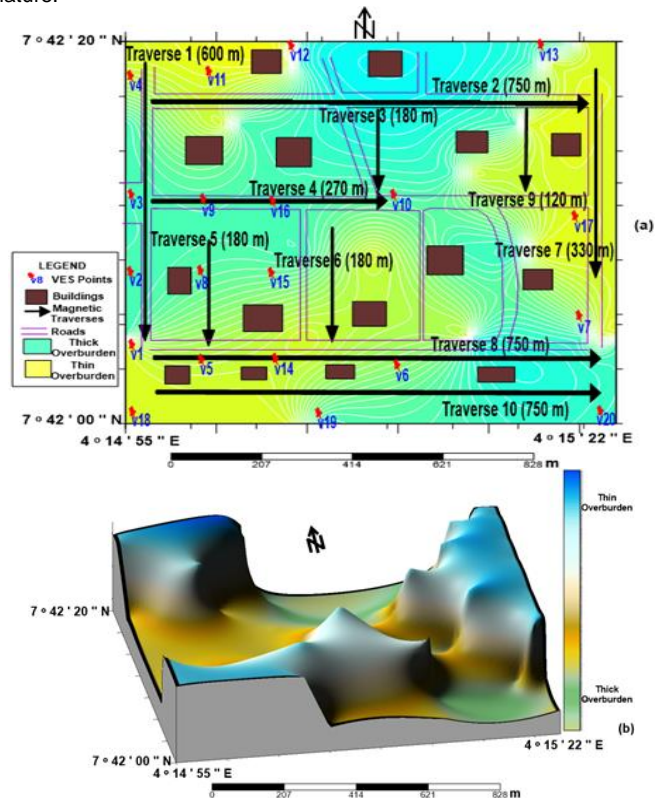


Fig. 12 (a) 2-D, and (b) 3-D: view of overburden thickness in the study area.

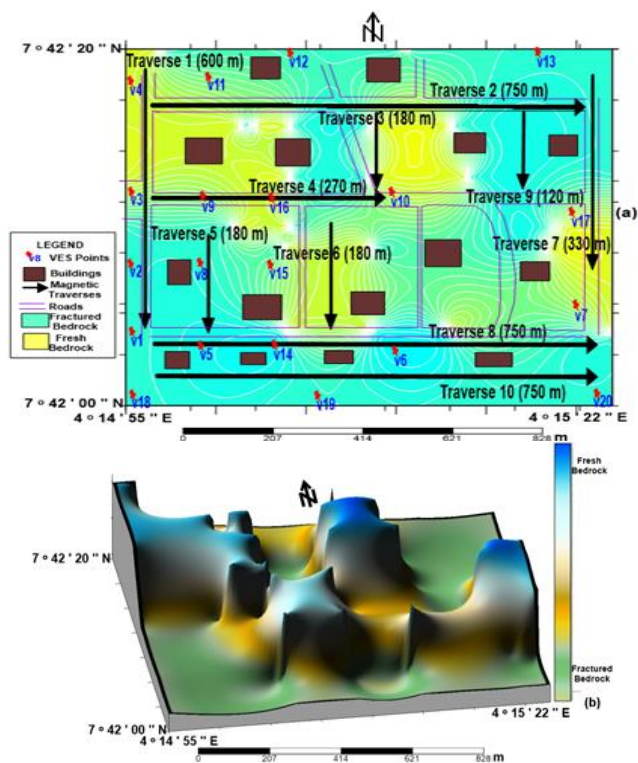


Fig. 13 (a) 2-D, and (b) 3-D: view of bedrock topography in the study area.

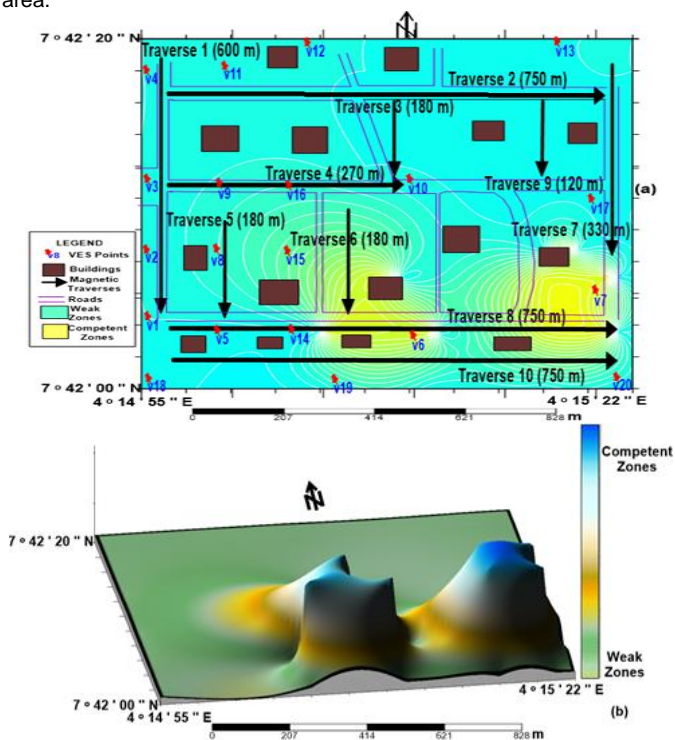


Fig. 14 (a) 2-D, and (b) 3-D: view of Subsurface Fabric Analysis map of the study area.

### Subsurface fabric analysis

The 2-D and 3-D subsurface fabric maps were generated based on the inference from geomagnetic and geoelectrical interpretations. It was affirmed that only the southern and some parts of southeastern region of the study area are competent for engineering purposes while about three-quarter of the study area is incompetent. The yellow colour on Fig. 14a represents the competent zones while the cyan colour represents the weak zones. These signatures are revealed on the 3-D subsurface fabric map of the study area (Fig. 14b). However, constructions of low-rise buildings are only advised on these weak

zones while high-rise buildings could be constructed on competent zones in the study area. These weak zones are better prospects for groundwater exploration because in Precambrian basement complex, thick overburden and fractured basement mostly favour groundwater exploration.

### CONCLUSION

Integration of ground magnetic and vertical electrical sounding techniques has proved very effective in geomapping of subsurface fabric in Awgbagba, southwestern Nigeria. This study has been able to map the competent zones for civil engineering and hydrogeological activities in Awgbagba. It was inferred from the study that only the southern and the southeastern parts of the study area are found suitable for civil engineering activities, other regions are considered as weak zones which could only accommodate low-rise building constructions. Groundwater exploration will be successful in Awgbagba if the weak zones identified were properly managed. However, for highly productive borehole development, the fracture zones mapped along parts of northeastern, northwestern and southwestern zones need to be utilized properly.

### REFERENCES

- Adagunodo, T. A., Sunmonu, L. A. 2012. Groundmagnetic survey to investigate on fault pattern of industrial estate Ogbomosho Southwestern Nigeria. *Advances in Applied Science Research* 3(5), 3142 – 3149.
- Adagunodo, T. A., Sunmonu, L.A., Adabanija, M. A. 2015a. Geomagnetic signature pattern of industrial layout Orile Igbon. *Advances in Architecture, City and Environment* 1(3), 14 – 25.
- Adagunodo, T.A., Adeniji, A.A., Erinle, A.V., Akinwumi, S.A., Adewoyin, O.O., Joel, E.S., Kayode, O.T. 2017. Geophysical investigation into the integrity of a reclaimed open dumsite for civil engineering purpose. *Interciencia Journal* 42(11), 324 – 339.
- Adagunodo, T.A., Sunmonu, L.A., Adeniji, A. A. 2015b. An overview of magnetic method in mineral exploration. *Journal of Global Ecology and Environment* 3(1), 13 – 28.
- Adagunodo, T.A., Sunmonu, L.A., Ojoawo, A., Oladejo, O.P., Olafisoye, E. R. 2013. The hydro geophysical investigation of Oyo State industrial estate Ogbomosho, Southwestern Nigeria using vertical electrical soundings. *Research Journal of Applied Sciences, Engineering and Technology* 5(5), 1816 – 1829.
- Adagunodo, T.A., Sunmonu, L.A., Oladejo, O. P. 2014. Effect of constructing high-rise buildings without a geophysical survey. *Nigerian Journal of Physics Special Edition September* 2014, 91 – 100.
- Adelusi, A.O., Akinlalu, A.A., Nwachukwu, A. I. 2013. Integration studies of buildings around school of science area, Federal University of Technology, Akure, Southwestern, Nigeria. *International Journal of Physical Sciences* 8(15), 657 – 669.
- Adewoyin, O.O., Joshua, E.O., Akinwumi, I.I., Omeje, M. and Joel, E. S. 2017. Evaluation of geotechnical parameters using geophysical data. *Journal of Engineering and Technological Sciences*. 49(1), 95 – 113.
- Al-Amoush, H. 2010. Integration of vertical electrical sounding and aeromagnetic data using GIS techniques to assess the potential of unsaturated zone and natural basalt caves for groundwater artificial recharge in NE-Jordan. *Jordan Journal of Civil Engineering* 4(4), 389 – 408.
- Al-Garni, M. A. 2009. Geophysical investigations for groundwater in a complex subsurface terrain, Wadi Fatima, KSA: A case history. *Jordan Journal of Civil Engineering* 3(2), 118 – 136.
- Al-Khafaji, W.M.S., Al-Dabbagh, H.A. Z. 2016. Visualizing geoelectric-Hydrogeological parameters of Fadak farm at Najaf Ashraf by using 2D spatial interpolation methods. *NRIAG Journal of Astronomy and Geophysics* 5(2), 313 – 322.
- Carruthers, R. M. 1985. Review of geophysical techniques for groundwater exploration in crystalline basement terrain. British Geological Survey. *Regional Geophysics Research Group, Report WK/RG/85/003*, 30 pp.
- Emenike, E. A. 2001. Geophysical exploration for groundwater in a sedimentary environment: a case study from Nanka over Nanka Formation in Anambra Basin, Southeastern Nigeria. *Global Journal of Pure and Applied Sciences* 7(1), 97 – 101.
- WinGLink software. Version 1.62.08 – 20030519. January 10, 2008. *Geosystem SRL*. Via Clericetti 42a, 20133 Milan, Italy.
- Hewaidy, A.G.A., El-Motaal, E.A., Sultan, S.A., Ramdan, T. M., El-Khafif, A. A., Soliman, S. A. 2015. Groundwater exploration using resistivity and

- magnetic data at the northwestern part of the Gulf of Suez, Egypt. *Egyptian Petroleum Research Institute* 24, 255 – 263.
- Keller, G. V., Frischnecht, F. C. 1966. *Electrical methods in geophysical prospecting*. New York: Pergamon Press, pp. 96.
- Koefoed, O. 1979. *Geosounding principles, 1. Resistivity measurements*. Amsterdam, Netherlands: Elsevier Scientific Publishing, pp. 275.
- Ojo, A.O., Omotoso, T.O., Adekanle, O. J. 2014. Determination of location and depth of mineral rocks at Olode village in Ibadan, Oyo State, Nigeria, using geophysical methods. *International Journal of Geophysics* Article ID 306862, 1 – 13.
- Okwoli, E., Onaja, O. S., Udoeyop, U. E. 2014. Ground magnetic and electrical resistivity mapping for basement structures over charnokitic terrain in Ado-Ekiti area, Southwestern Nigeria. *International Journal of Science and Technology* 3(10), 683 – 689.
- Olayanju, G.M., Adelusi, A.O., Adiat, K. A. 2015. Combined use of ground magnetic and electrical resistivity methods in bedrock mapping: case study of NTA premises Oba Ile area, South-western Nigeria. *EJGE* 20(15), 6591 – 6606.
- Oyeyemi, K.D., Aizebeokhai, A.P., Adagunodo, T.A., Olofinnade, O.M., Sanuade, O.A., Olajojo, A.A. 2017. Subsoil characterization using geoelectrical and geotechnical investigations: implications for foundation studies. *International Journal of Civil Engineering and Technology* 8(10), 320 – 314.
- Sunmonu, L.A., Adagunodo, T.A., Olafisoye, E. R., Oladejo, O. P. 2012. The groundwater potential evaluation at Industrial Estate Ogbomoso, southwestern Nigeria. *RMZ – Materials and Geoenvironment* 59(4), 363 – 390.
- Surfer 11 software. Version 11.0.642. July, 2012. *Golden Software, Inc.*, 809 14<sup>th</sup> street Golden, Colorado, 80401 – 1866, U.S.A.
- Telford, W.M., Geldart, L. P., Sheriff, R. E. 1976. *Applied Geophysics* (2<sup>nd</sup> Ed.) Cambridge: Cambridge University Press.
- Vander Velpen, B. P. A. 2004. *WinRESIST Software Version 1.0. ITC, ITRSG/GSD*, Delft, Netherlands.